Preprint typeset using LaTeX style emulateapj v. 08/13/06

AN INVESTIGATION OF THE ENVIRONMENTS OF GRAVITATIONAL LENS SYSTEMS WITH KNOWN TIME DELAYS

Allison Arpin
Elon University

ABSTRACT

The local environments for 17 strong gravitational lens systems with known time delays and values for the Hubble Constant are analyzed. The data reduction process for WFPC2, ACS, and NICMOS, the three HST cameras used to collect data, is described. A preliminary analysis counting the number of companion galaxies within a certain radial distance from the lensing galaxy is performed. The method for determining the redshift of the field galaxies photometrically is presented. Weighting the offset and the probable redshift will lead to a determination of the number of field galaxies that are physically associated with the lensing galaxy and whether or not there is a trend between the number of companion galaxies and the estimation of the Hubble Constant.
Subject headings:

1. BACKGROUND

Gravitational lensing, the deflection of light by massive bodies, has a number of different uses in astrophysics. Lensing acts as a type of cosmic telescope, magnifying faint or distant galaxies that would otherwise remain unseen. Gravitational lensing can also be used to study the distribution of both baryonic and dark matter in the universe, and lensing statistics help constrain cosmological models. Strong gravitational lenses produce multiple images of quasars that have a distinct image separation, flux ratio, and time delay. Knowing these parameters limits the freedom of the cosmological models.

Knowing the time delay between images also provides a way in which to measure the Hubble Constant (Refsdal 1964). This measurement depends on the slope of the mass distribution of the lensing galaxy. A steeper profile will result in a higher value measured for the Hubble Constant, while a shallower profile will result in a lower value. An isothermal mass profile ($\rho \propto r^{-2}$) is often used to model the lensing galaxy, but the use of such a profile in one sample of lenses produces a wide range of values measured for the Hubble Constant (Oguri 2007). There is an accepted value for the Hubble Constant from the HST Key Project ($H_0 = 72 \pm 8\,\mathrm{km\,s^{-1}Mpc^{-1}}$; Freedman et al. 2001) that is considered robust. Since a number of lens systems in the Oguri analysis either underestimate or overestimate H_0 compared to the Key Project value, it is possible that not all lensing galaxies should be modeled with an isothermal mass profile. In particular, lenses giving values of H_0 lower than the Key Project value may have mass profiles that are steeper than the assumed isothermal mass profile.

Results from Dobke (2007) suggest that galaxies which undergo galaxy-galaxy interactions might be better modeled with a steeper than isothermal mass profile. Thus, there may be a correlation between the value measured for the Hubble Constant for a lensing galaxy and the number of companions that reside near that galaxy. Auger et al. (2007a) suggest that one lens system, SBS1520+530, which is known to have both a galaxy companion and a low measured Hubble Constant does seem to fit well within a steeper profile. A photometric analysis of a sample of lens systems with known density profiles from the Sloan Lens ACS Survey (SLACS; Bolton et al. 2006) also indicates a trend that lens systems with companions follow a steeper mass profile (Auger 2007b), where the mass profile is determined by measuring the mass of the galaxies at several radii (Koopmans et al. 2006). Though the trend seems strong, there was one lens with a steeper than isothermal mass profile in the SLACS sample that did not have any companion galaxies, suggesting that either a photometric analysis is inadequate or that there are other factors that need to be taken into consideration in the models (Auger 2007b). This warrants an investigation of more lens systems to determine whether the trend is supported even further.

This paper summarizes the process leading to an analysis of a sample of 17 strong gravitational lens systems with known time delays and predicted values for the Hubble Constant as reported by Oguri (2007). In Section 2 the method for the reduction of data is presented. In Section 3 the method for the analysis is proposed, and

in Section 4 future work is discussed.

2. DATA REDUCTION

Data for 16 out of the 17 lens systems reported on by Oguri (2007) were retrieved from the Hubble Space Telescope (HST) archive.[1] SDSS1650+4251 had no data in the archive, therefore it was omitted from the sample. Q0957+561 and PKS1830-211 were also omitted from the sample due to the complexity from residing in a galaxy cluster and having a low galactic latitude, respectively.

Three different cameras from the HST were used to collect data: The second Wide Field Planetary Camera (WFPC2), the Advanced Camera for Surveys (ACS) and the Near Infrared Camera and Multi-Object Spectrometer (NICMOS). WFPC2 is comprised of four charge coupled devices (CCDs). Three of these are wide field chips and one is a planetary chip. All four chips contain the same number of pixels, but the planetary chip covers a smaller area, thus creating a more detailed image.

ACS covers twice the area of WFPC2 and contains three different cameras: A solar blind camera which is sensitive to ultraviolet light, a wide field camera, and a high-resolution camera. The ACS data from the sample of 14 lens systems was taken from the wide field camera.

Like ACS, NICMOS also contains three cameras; NIC2 was the camera from which data was taken for the current sample of lenses. The three NICMOS cameras create images of objects in the near-infrared wavelengths. Consequently, the camera must be cooled to cryogenic temperatures in order to minimize the thermal background of the instrument.

Images from WFPC2 are first reduced by an IRAF script, *multidrizzle*. When images are taken by the HST, the camera is often dithered, or moved slightly in a pattern to avoid having bad pixels in the same place on each image. After retrieval from the HST archives, the dithered images must be combined. In general *multidrizzle* performs this task well using the internal calibrations of HST to three stars with known positions. Occasionally, though, there is a significant time lapse between imaging or there is a large difference in position angle between two images; this may cause a different set of three stars to be used and consequently the coordinate frame to shift slightly. In these cases *multidrizzle* is often not able to combine the dithered images correctly, and images taken at different times or position angles must be drizzled separately.

While the HST is taking data, the instrument is often hit by highly energetic charged particles called cosmic rays. This produces light pixels and streaks in the images. A second function of *multidrizzle* is to reject these cosmic rays from the images. There is a low probability that a cosmic ray will be found in the same pixel for every image. *Multidrizzle* compares each image and corrects the pixels where cosmic rays are found.

A catalog of objects and galaxy properties

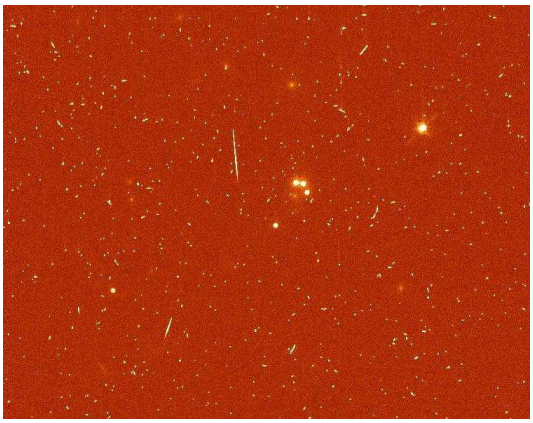

FIG. 1.— A HST image of RXJ0911+0551 before multidrizzling. The bright dots and streaks are due to cosmic rays.

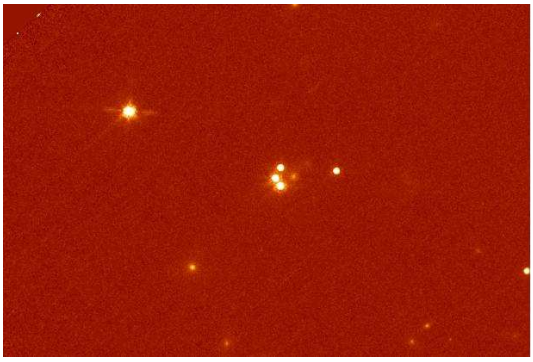

FIG. 2.— A HST image of RXJ0911+0551 after multidrizzling. The cosmic rays have been rejected and the position angle has been altered.

from each drizzled image was created using SExtractor (Bertin & Arnouts 1996). Since the drizzled images are often not matched to the same astrometry due to the incorrect calibrations of HST, objects must be matched to an outside catalog in order to place all of the drizzled images onto one common coordinate frame. The catalog of objects created by SExtractor from each drizzled image was matched to an astrometric catalog from either the Sloan Digital Sky Survey (SDSS) or the latest catalog from the United States Naval Observatory (USNO-B1). Since the SDSS catalog is deeper than USNO-B1, it was used when available; however, SDSS only covers a quarter of the sky, so there were situations when no sources from SDSS fell in the same field

[1] http://archive.stsci.edu/hst/

of view. In those cases, USNO-B1, which provides all sky coverage, was used.

The updated images were resampled using SWarp, which creates a final coadded image for each filter using an astrometric projection. A final catalog of objects and galaxy properties for each coadded image was made with SExtractor.

Most of the ACS images were reduced by the HST Archive Galaxy-scale Gravitational Lens Survey (HAGGLeS) at Stanford. The rest of the ACS images were reduced using the same method as the WFPC2 images. Those lens systems that were not reduced by HAGGLeS are B0218+357, HE0435-1223, and RXJ1131-1231.

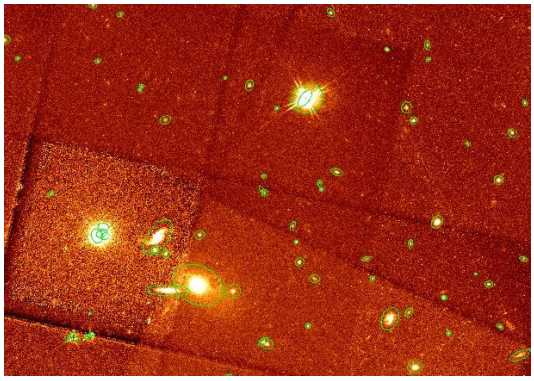

FIG. 3.— A HST image of PG1115+080 with the objects detected by SExtractor circled in green.

Images from NICMOS were reduced in the same way as the WFPC2 images with one exception. Instead of matching the images to either the SDSS or UNSO-B1 astrometric catalogs, the NICMOS images for each lens system were matched to the final WFPC2 or ACS catalog of objects created by SExtractor. The NICMOS images are so small that there are few sources in either SDSS or USNO-B1 to match with. Consequently, a better match is made using the catalogs created by SExtractor.

During the reduction process, the field of HE1104-1805 was too sparse for many sources from SDSS or USNO-B1 to match. Since no ground based imaging for the lens system is available with which to match objects, it was omitted from the sample. The final sample therefore consists of 13 lens systems. The redshift of the lensing galaxy and the estimated Hubble Constant for each system are recorded in Table 1.

3. ANALYSIS

The first step is to count the number of galaxies within some radial distance of the lens to determine if there are any neighboring galaxies. The distance chosen is $10''$ of the lensing galaxy. A catalog was created of all objects that fall within that radius. Only galaxies that are between one magnitude brighter and 2.5 magnitudes fainter than the lensing galaxy were included in the catalog. This preliminary step is currently the only one complete in the analysis. Figure 4 compares the Hubble Constant with the number of neighboring galaxies counted. The dashed line represents $H_0 = 72 \pm 8\,\mathrm{km\,s^{-1}Mpc^{-1}}$.

There does not seem to be a trend between the value reported for H_0 and the number of companion galaxies counted. Since only galaxies at a similar redshift to the lensing galaxy will affect the mass profile, the redshift of the field galaxies must also be taken into account. Discarding field galaxies that are not at the redshift of the lensing galaxy may produce a stronger trend.

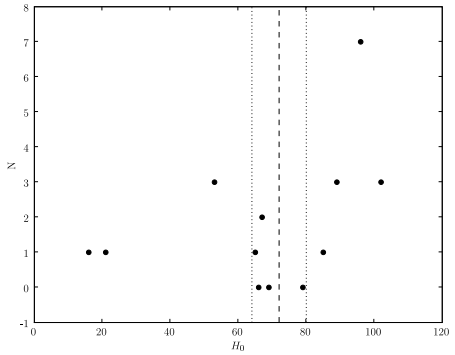

FIG. 4.— The number of neighboring galaxies (N) versus the value reported for the Hubble Constant (H_0). The dashed line represents $H_0 = 72$ and each dotted line represents the error in the Key Project value at $H_0 = 64$ and $H_0 = 80$. There is no evidence for a trend.

Since spectra are not available for each lens system, a photometric analysis needs to be performed to determine the redshift of each field galaxy. Galaxy colors will be used to determine whether a galaxy is at the same redshift as the lens. Rather than determining the photometric redshift, which gives the most probable redshift for a source, the probability that a source is at the redshift of the lens will be determined using the weighting scheme from Auger (2007b). The weighting takes into account both the distance of each source from the lens and the color distributionsof galaxies at the same redshift as the lens; a sum over the weights produces a final number of galaxies that are physically associated with the lensing galaxy. The number of companion galaxies will again be compared with the reported Hubble Constant for each lens system to determine if there is a trend.

TABLE 1
Lens redshift and Hubble Constant for the sample of 13 lens systems

Name	z_l *	H_0 (1σ range) *	Analyzed
B0218+357	0.685	21 (-)	Y
B1422+231	0.337	16 (- 36)	Y
B1600+434	0.414	65 (54 - 77)	Y
B1608+656	0.630	89 (77 - 120)	Y
FBQ0951+2635	0.260	67 (56 - 81)	Y
HE0435-1223	0.455	102 (70 - 139)	Y
HE1104-1805	0.729	104 (92 - 122)	N
HE2149-2745	0.603	69 (57 - 82)	Y
PKS1830-211	0.89	88 (58 -)	N
PG1115+080	0.310	66 (49 - 84)	Y
Q0957+561	0.36	99 (82 - 117)	N
RXJ0911+0551	0.769	96 (75 - 121)	Y
RXJ1131-1231	0.295	79 (59 - 103)	Y
SBS0909+523	0.830	85 (47 -)	Y
SBS1520+530	0.717	53 (46 - 61)	Y
SDSS J1004+4112	0.68	N/A	Y
SDSS J1650+4251	0.577	53 (44 - 63)	N

*Data from Oguri (2007).

4. DISCUSSION

With the information currently available, it is not possible to conclude whether the lenses in the sample that are better modeled with a steeper than isothermal mass profile reside near companion galaxies. The preliminary analysis did not indicate that lenses with lower reported values for the Hubble Constant had more companion galaxies than lenses that overestimated or correctly estimated H_0. Once a photometric color distribution is created for each lens system and the correct number of companion galaxies is calculated using the weighting scheme, it will be possible to conclude whether or not a trend appears for this sample of lenses.

Once the photometric analysis is complete, it would be worthwhile to obtain spectra for the sample of lensing galaxies. An analysis using spectometry would provide a more accurate and precise measurement of the redshift for each field galaxy and would eliminate the need for a weighting scheme.

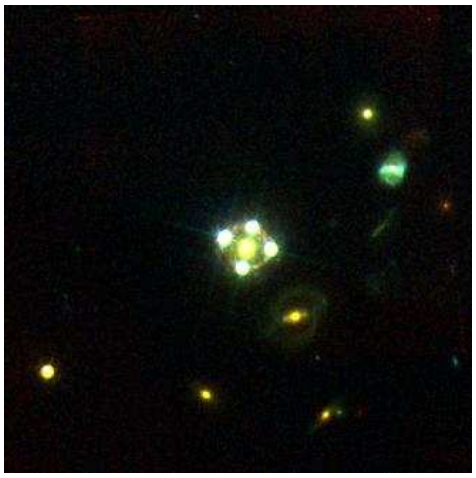

Fig. 5.— A color image of HE0435-1223.

ACKNOWLEDGMENTS

I would like to thank Chris Fassnacht and Matt Auger for their guidance in this project. This work was supported by the National Science Foundation and the UC Davis physics REU program.

REFERENCES

Auger, M. W., Fassnacht, C. D., Wong, K. C., Thompson, D., Matthews, K., & Soifer, B. T. 2007a, submitted to ApJ

Auger, M. W. 2007b, submitted to MNRAS

Bertin, E., & Arnouts, S. 1996, A&AS, 117, 393

Bolton, A. S., Burles, S., Koopmans, L. V. E., Treu, T., & Moustakas, L. A., 2006, ApJ, 638, 703

Dobke, B. M., King, L. J., & Fellhauer, M. 2007, MNRAS, 377, 1503

Freedman, W. L., et al. 2001, ApJ, 553, 47

Koopmans, L. V. E., Treu, T., Bolton, A. S., Burles, S., & Moustakas, L. A., 2006, ApJ, 649, 599

Oguri, M. 2007, ApJ, 660, 1

Refsdal, S. 1964, MNRAS, 128, 307